ORIGINAL ARTICLE

Safflor Yellow A Protects Beas-2B Cells Against LPS-Induced Injury via Activating Nrf2

Liang-Shu Chen[1] · **Dong-Shu Zheng**[2,3,4]

Abstract

Acute lung injury and its severe form acute respiratory distress syndrome are lethal lung diseases. So far, effective therapy for the diseases is deficient and the prognosis is poor. Recently, it was found activating nuclear factor erythroid 2-related factor 2 could attenuate the injury including inflammation, oxidative stress, and apoptosis in those diseases. To discover novel therapy, we have evaluated safflor yellow A and explored the underlying mechanisms using Beas-2B cells injured by lipopolysaccharide. As a result, safflor yellow A could improve the viability of Beas-2B cells treated with lipopolysaccharide. Further investigations have revealed safflor yellow A suppressed oxidative stress induced by lipopolysaccharide via reducing reactive oxygen species and malondialdehyde, and elevating superoxide dismutase, catalase, and glutathione peroxidase. Meanwhile, the inflammation resulting from lipopolysaccharide was ameliorated through decreasing the pro-inflammatory cytokines including tumor necrosis factor-α, interleukin-1β, and interleukin-6. It was also found nuclear factor κB was inactivated by safflor yellow A. In addition, safflor yellow A downregulated cysteinyl aspartate specific proteinase-3 and Bcl-2-associated X protein and upregulated B-cell lymphoma-2 to inhibited apoptosis of Beas-2B cells induced by lipopolysaccharide. The activation of nuclear factor erythroid 2-related factor 2 was observed in Beas-2B cells, which was associated with the protective effects of safflor yellow A. And molecular docking elucidated safflor yellow A interacted with Kelch-like ECH-associated protein 1 to activate nuclear factor erythroid 2-related factor 2. These results can provide evidences for the discovery of novel therapy for further evaluation of safflor yellow A in the treatment of acute lung injury and acute respiratory distress syndrome.

Keywords *Carthamus tinctorius* · Natural products · Lung disease · Bronchial epithelial cells

Introduction

Acute lung injury (ALI) and the following acute respiratory distress syndrome (ARDS) are lethal lung diseases with high morbidity and mortality (Liu et al. 2022a). Direct pulmonary insults and indirect inflammatory responses resulting from sepsis, trauma, and major surgery related to pulmonary infection are the major causes of ALI/ARDS (Fan and Fan 2018). In clinics, the primary treatment for ALI/ARDS mainly focuses on symptomatic therapy including mechanical ventilation and fluid management. However, due to the lack of effective therapeutic strategies, the prognosis for most ALI/ARDS patients is despondent (Liu et al. 2022b). The pathogenesis of ALI/ARDS has revealed inflammation plays a pivotal role (Mokrá 2020). In addition, oxidative stress and apoptosis were also observed in the progression of ALI/ARDS (Imai et al. 2008; Galani et al. 2010).

Nuclear factor erythroid 2-related factor 2 (Nrf2) is a transcription factor affording the regulation of some genes via binding to antioxidant response elements (ARE) in their promoter regions (Torrente and DeNicola 2022). Under basal condition, Nrf2 is captured in cytosol by Kelch-like ECH-associated protein 1 (Keap1) and degraded by 26S proteasome after ubiquitination (Bryan et al. 2013). However, in

✉ Dong-Shu Zheng
zhengdsxm@sina.com

[1] Ward of Healthcare Branch II, The First Affiliated Hospital of Xiamen University, Xiamen 361003, Fujian, China

[2] The Third Clinical Medical College, Fujian Medical University, Xiamen 361003, Fujian, China

[3] Department of Otolaryngology, Head and Neck Surgery, The First Affiliated Hospital of Xiamen University, No. 55 Zhenhai Road, Xiamen 361003, Fujian, China

[4] Xiamen Key Laboratory of Otolaryngology, Head and Neck Surgery, Xiamen 361003, Fujian, China

the presence of oxidants or electrophiles, the interaction between Keap1 and Nrf2 is disrupted and Nrf2 translocates into nucleus from cytosol, which resulted in its activation (Yamamoto et al. 2018). The activated Nrf2 can bind to the ARE of target genes to promote the expression of the antioxidant and detoxified enzymes such as heme oxygenase-1 (HO-1), NAD(P)H:quinone oxidoreductase 1 (NQO1), superoxide dismutase (SOD), catalase (CAT), and glutathione peroxidase (GSH Px) (Shaw and Chattopadhyay 2020). Therefore, activating Nrf2 gives a potential approach to attenuate oxidative stress-related diseases (Cuadrado et al. 2019). Meanwhile, it is approved activation of Nrf2 could ameliorate inflammation through multiple pathways (Keleku-Lukwete et al. 2018). Recently, it has been raised that activation of Nrf2 could attenuate respiratory diseases including ALI/ARDS (Rojo de la Vega et al. 2016; Lee et al. 2021).

In the discovery of a Nrf2 activator, phytochemicals play a pivotal role (Wu et al. 2022). Some natural compounds such as vincamine, sophoricoside, and diosmetin could attenuate ALI via activating Nrf2 (Liu et al. 2018; Wu et al. 2021; Patangrao Renushe et al. 2022). Safflor yellow A (**1**) is the major phytochemical found in *Carthamus tinctorius* L., Asteraceae (Takahashi et al. 1982). As a chalcone derivative, it showed antioxidant activity and protective effects on human umbilical vein endothelial cells and rat cardiomyocytes against oxidative stress and apoptosis (Duan et al. 2013; Bacchetti et al. 2020; Zhang et al. 2022). In our interests in searching a natural Nrf2 activator for the treatment of ALI/ARDS, we have explored the protective effects of safflor yellow A on human lung bronchial epithelial Beas-2B cells against the injury induced by lipopolysaccharide (LPS) and underlying mechanisms.

1
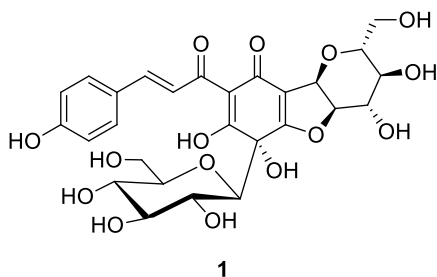
Materials and Methods

Chemicals and Reagents

Safflor yellow A (purity ≥ 98%, lot No. 157723) was provided by TargeMol (Wellesley Hills, MA). 3-[4,5-Dimethylthiazol-2-yl]-2,5-diphenyltetrazolium bromide (MTT), LPS, and sulforaphane (SFN) were purchased from Sigma-Aldrich (St. Louis, MO). ML385 was obtained from Meilunbio (Dalian, China). ROS assay kit, 4′,6-diamidino-2-phenylindole (DAPI) staining solution, bicinchoninic acid (BCA) protein assay kit, nuclear and cytosolic protein extraction kit, SOD activity assay kit, CAT activity assay kit, GSH Px activity assay kit, malondialdehyde (MDA) assay kit, and horseradish peroxidase conjugated secondary antibody, enhanced chemiluminescence (ECL) assay kit together with enzyme-linked immunosorbent assay (ELISA) kits including tumor necrosis factor-α (TNF-α), interleukin-1β (IL-1β), and interleukin-6 (IL-6) were provided by Beyotime Biotechnology Institute (Shanghai, China). The ELISA kits for HO-1 and NQO1 were products of Colorfulgene Biotechnology (Wuhan, China). The primary antibodies for cleaved cysteinyl aspartate specific proteinase-3 (cleaved caspase-3) (AF7022), cysteinyl aspartate specific proteinase-3 (caspase-3) (AF6311), B-cell lymphoma-2 (Bcl-2) (AF6139), and Bcl-2-associated X protein (Bax) (AF0120) were supplied by Affinity Biosciences (Cincinnati, OH). And others including phosphorylated nuclear factor κB p65 (p-NF-κB p65) (ab76302), nuclear factor κB p65 (NF-κB p65) (ab32536), phosphorylated inhibitor of NF-κB α (p-IκBα) (ab133462), inhibitor of NF-κB α (IκBα) (ab32518), Nrf2 (ab92946), GAPDH (ab9485), and lamin B1 (ab16048) together with DyLight594 conjugated secondary antibody (ab96885) were obtained from Abcam (Cambridge, UK).

Cell Culture and Treatment

Human lung bronchial epithelial Beas-2B cells were obtained from American Type Culture Collection (ATCC) and maintained in DMEM supplemented with 10% fetal bovine serum (FBS) and 1% penicillin/streptomycin at 37 °C under a humid condition of 5% CO_2. Cells were set as control group, LPS group, and drug groups. The LPS group was exposed to 0.1 mg/ml LPS in DMEM for 24 h. In addition to 100 μg/ml LPS, the drug groups were incubated with certain SYA or SFN for 24 h. The cells in the control group were cultivated in normal DMEM.

Cell Viability

Beas-2B cells were seeded in 96-well culture microplates at the density of 5×10^3 cells per well. After treated as above 20 μl MTT solution (5 mg/ml) were added and incubated for 4 h. Then, the medium was removed and 200 μl DMSO was added to dissolve the formazan crystals. The absorbance was determined on a microplate reader (BioTek, Winooski, VT) at 570 nm. To present the trends of cell viability, the concentrations of SYA were expressed as logarithm.

ROS Production

To detect the ROS level in Beas-2B cells, DCFH-DA in the assay kit was employed. In brief, the cells were treated as above and then exposed to DCFH-DA (0.5 mg/ml) for 20 min. The fluorescence intensity was read on a fluorescence microplate (Molecular Devices, San Jose, CA) with the excitation wavelength of 488 nm and emission wavelength of 525 nm.

MDA Content

The MDA content in Beas-2B cells was detected using a commercially available assay kit. According to the supplier's instruction, the cells were treated as above and lysed on ice. After centrifugation at $1600 \times g$, the supernatant was collected and exposed to the working solution in the assay kit. Then the sample was boiled for 15 min and cooled to room temperature. The absorbance was recorded on a microplate reader at 532 nm.

SOD, CAT, and GSH Px Activity

To detect the activity of SOD, CAT, and GSH Px in Beas-2B cells, the colorimetric method was employed using the commercially available assay kits. In brief, the treated cells were homogenized at 4 °C and the supernatant was collected as samples for further analysis after centrifugation at $12,000 \times g$ and 4 °C for 10 min. Then the protein concentration was quantified using a BCA assay kit, and enzyme activity was determined according to the supplier's protocols on a microplate reader.

Immunofluorescence Staining

To reveal the location of intracellular Nrf2 in Beas-2B cells, immunofluorescence staining was performed. The cells were seeded in 12-well microplates with a coverslip in each well and treated as above indication. Then the cells were fixed with 4% paraformaldehyde and permeated with PBS containing 0.1% Triton X-100. Then the cells were exposed to the primary antibody of Nrf2 (1:200) overnight. DyLight594 conjugated secondary antibody was used to detect the protein. After staining with DAPI in the dark, the images were captured using a Nikon fluorescence microscope (Tokyo, Japan).

ELISA

To uncover the levels of TNF-α, IL-1, IL-6, HO-1, and NQO1 in Beas-2B cells, ELISA was implemented using the assay kits. For the secretion of pro-inflammatory cytokines, the treated cells were centrifuged at $500 \times g$ for 5 min and the supernatant was collected for further analysis. For the intracellular enzymes, the treated cells were lysed at 4 °C and then the supernatant was also collected following centrifugation at $1000 \times g$ for 20 min. Then the samples were handled in light of the suppliers' protocols, and the absorbance was recorded on a microplate reader at 450 nm.

Western Blot Analysis

The total proteins were extracted using RIPA lysis buffer while the nuclear proteins were obtained using the nuclear and cytosolic protein extraction kit according to the supplier's instructions. The protein concentrations were determined using BCA protein assay kit, and the proteins were separated on 10% SDS-PAGE and transferred to PVDF membranes. After blocking with non-fat milk, the membranes were incubated with primary antibodies including cleaved caspase-3 (1:1000), caspase-3 (1:1000), Bcl-2 (1:1000), Bax (1:1000), p-IκBα (1:10,000), IκBα (1:1000), p-NF-κB p65 (1:1000), NF-κB p65 (1:1000), Nrf2 (1:1000), GAPDH (1:2500), and lamin B1 (1:1000) at 4 °C overnight. After being rinsed with TBST buffer, the membranes were cultured with horseradish peroxidase conjugated secondary antibodies at room temperature for 1 h. The bands were visualized using an ECL substrate on a Bio-Rad imaging system (Hercules, CA). GAPDH and lamin B1 were used as internal controls. ImageJ software (NIH, Bethesda, MD) was used for densitometric analysis.

Molecular Docking

To elucidate the effect of safflor yellow A on Keap1-Nrf2 interaction, molecular docking was performed as our previous description (Zheng and Chen 2017). In brief, the 3D structure of safflor yellow A was established on SYBYL sketch and optimized by Tripos force field and Gasteiger-Huckel charges. The crystal structure of Keap1 Kelch domain was obtained from RSCB Protein Data Bank (PDB code: 4IQK). The protomol file was generated to produce the docking envelope and Surflex-Dock program with default parameters was operated for docking calculations.

Statistical Analysis

The data was provided as mean ± standard deviation and analyzed by GraphPad Prism 8.0 (San Diego, CA). The differences among groups were assessed using one-way analysis of variance (one-way ANOVA) followed by the Tukey test for multiple comparisons and Student's t test for single comparisons. A $p < 0.05$ was considered significant in statistics.

Results

Safflor Yellow A Improves the Survival of Beas-2B Cells Injured by LPS

As shown in Fig. 1A, safflor yellow A cannot affect the survival of normal Beas-2B cells even at 100 µM. After treatment with LPS (0.1 mg/ml), the cell viability was decreased sharply ($p < 0.01$) while in the presence of safflor yellow A from 1 µM (expressed as logarithm), the poor cell viability was improved significantly ($p < 0.05$) (Fig. 1B), which gave the indication for the following exploration.

Safflor Yellow A Attenuates Oxidative Stress Induced by LPS in Beas-2B Cells

To elucidate the protective effects of safflor yellow A against the injury induced by LPS, we have detected the oxidative stress in Beas-2B cells. Compared to control group, LPS has caused the overproduction of ROS ($231.8 \pm 11.9\%$) and MDA ($289.6 \pm 13.3\%$). However, safflor yellow A at 5 µM could reduce both ROS ($140.4 \pm 7.4\%$) and MDA ($166.8 \pm 11.4\%$), respectively. At the same time, ML385, the specific Nrf2 inhibitor, can block the effects of safflor yellow A and result in the decreasing ROS ($218.7 \pm 7.4\%$) and MDA ($279.6 \pm 7.8\%$) (Fig. 2A and B). In addition, the activity of antioxidant enzymes including SOD, CAT, and GSH Px in Beas-2B cells was measured herein. After exposure to LPS, the activity of SOD, CAT, and GSH Px was inhibited as $52.1 \pm 6.8\%$, $61.5 \pm 6.1\%$, and $50.8 \pm 7.7\%$, respectively. Following the addition of safflor yellow A at 5 µM, it was observed that the activity of SOD, CAT, and GSH Px was elevated as $88.7 \pm 6.4\%$, $86.3 \pm 5.5\%$, and $87.7 \pm 6.9\%$, respectively, whereas ML385 could prevent the effects of safflor yellow A and lead to the decreasing activity of SOD ($59.6 \pm 9.4\%$), CAT ($67.4 \pm 5.4\%$), and GSH Px ($61.7 \pm 6.0\%$) (Fig. 2C–E).

Safflor Yellow A Ameliorates Inflammation Induced by LPS in Beas-2B Cells via Blocking NF-κB Signaling Pathway

To explore the inflammation in Beas-2B cells, pro-inflammatory cytokines such as TNF-α, IL-1β, and IL-6 were measured. The results showed LPS induced the excessive secretion of TNF-α ($607.5 \pm 17.3\%$), IL-1β ($676.6 \pm 12.6\%$), and IL-6 ($443.1 \pm 10.1\%$) compared with the control group. Safflor yellow A could reduce the synthesis of TNF-α ($182.2 \pm 13.9\%$), IL-1β ($192.2 \pm 17.6\%$), and IL-6 ($175.7 \pm 8.4\%$) significantly. But ML385 has resulted in the decreasing effects of safflor yellow A on TNF-α ($573.3 \pm 14.9\%$), IL-1β ($650.4 \pm 11.2\%$), and IL-6 ($430.3 \pm 7.9\%$) (Fig. 3A–C). Meanwhile, western blot analysis has revealed LPS promoted the phosphorylation of both IκBα and NF-κB while safflor yellow A could suppress this phosphorylation, which can be reversed by ML385 (Fig. 3D). The densitometric analysis also unraveled these results accordingly (Fig. 3E and F).

Safflor Yellow A Inhibits Apopotosis of Beas-2B Cells Induced by LPS

The apoptosis of Beas-2B cells induced by LPS was detected herein. As shown in Fig. 4A, the expression of cleaved caspase-3 was upregulated by LPS together with pro-apoptotic Bax, while the anti-apoptotic Bcl-2 was downregulated. In the presence of safflor yellow A, it was observed both cleaved caspase-3 and Bax were downregulated markedly, but Bcl-2 was upregulated. However, after exposure to ML385, the effects of safflor yellow A on cleaved caspase-3, Bcl-2, and Bax were repressed remarkably. Further densitometric analysis has also validated the results quantitatively (Fig. 4B–D).

Fig. 1 Effects of safflor yellow A (**1**) on the viability of Beas-2B cells with or without LPS. **A** Viability of normal Beas-2B cell with different concentrations of safflor yellow A. **B** Viability of Beas-2B cell induced by LPS with different concentrations of safflor yellow A. $n = 3$, $*p < 0.05$ vs LPS group
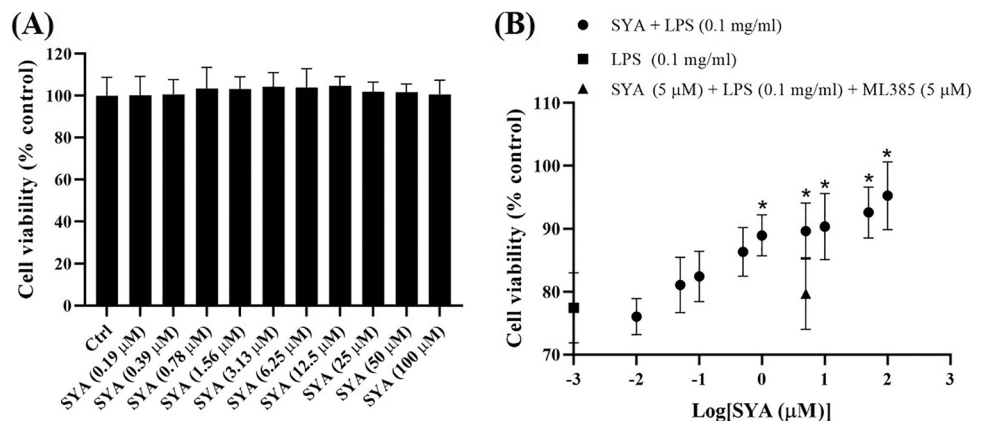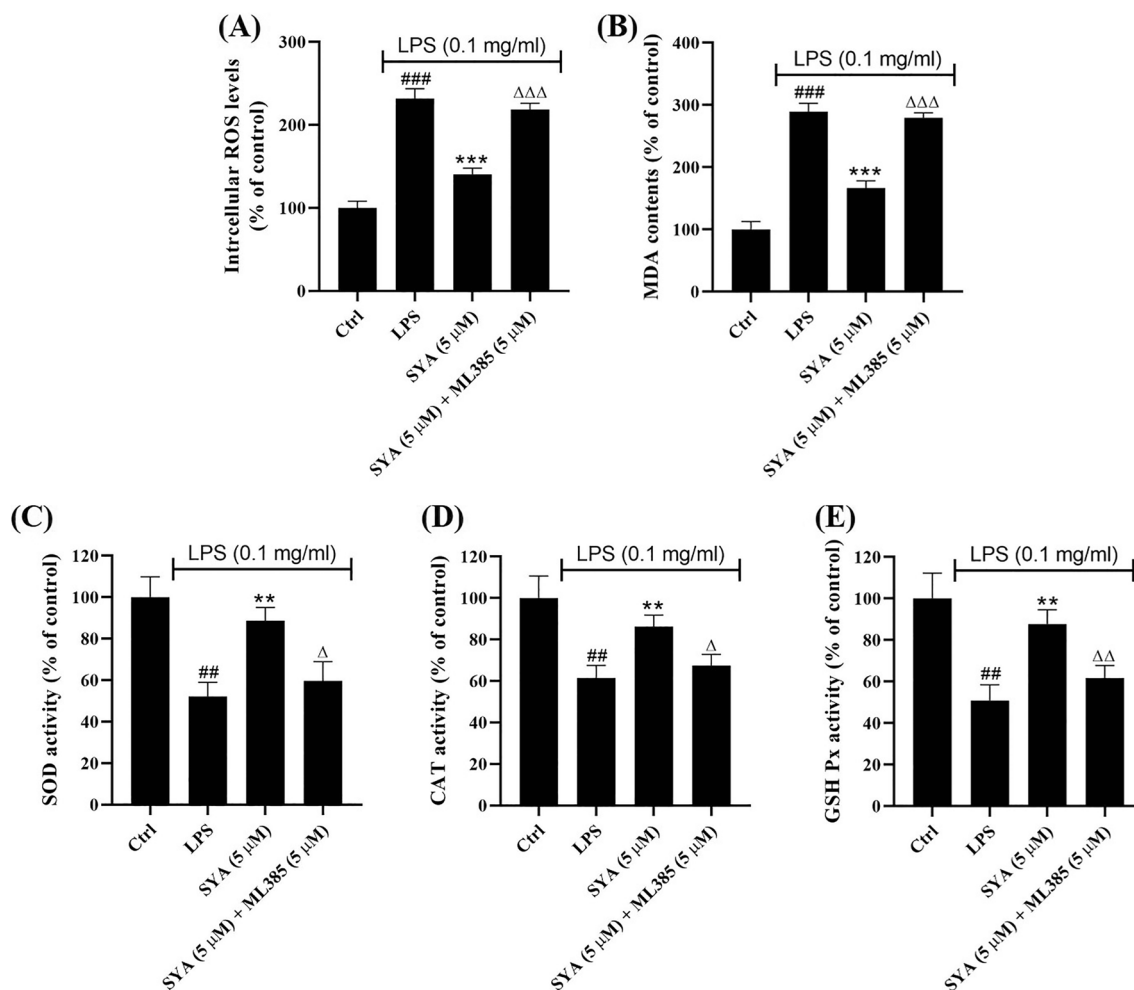
Fig. 2 Effects of safflor yellow A (**1**) on oxidative stress caused by LPS in Beas-2B cells. **A** Intracellular ROS level. **B** MDA content. **C–E** Activity of SOD, CAT, and GSH Px. $n = 3$, $^{##}p < 0.01$ and $^{###}p < 0.001$ vs control group, $^{**}p < 0.01$ and $^{***}p < 0.001$ vs LPS group, $^{\Delta}p < 0.05$, $^{\Delta\Delta}p < 0.01$, and $^{\Delta\Delta\Delta}p < 0.001$ vs SYA group

Safflor Yellow A Activates Nrf2 in Beas-2B Cells Injured by LPS in a Keap1-Dependent Manner

To reveal the mechanisms of safflor yellow A, Nrf2 in Beas-2B cells was investigated herein. As shown in Fig. 5A as the arrow indicated, immunofluorescence assay has indicated safflor yellow A enhanced the translocation of Nrf2 into nuclei from cytosol. Meanwhile, western blot analysis together with densitometric analysis for nuclear and total Nrf2 has implied safflor yellow A elevated their levels in Beas-2B cells treated with LPS (Fig. 5B–D), which implicated the activation of Nrf2. To further confirm the transcription capacity of activated Nrf2, NOQ1 and HO-1 were explored. As a result, LPS lessened NOQ1 and HO-1 levels which were reversed by safflor yellow A similar to sulforaphane, which suggested the activation of Nrf2. To visualize the Nrf2 activation in detail, molecular docking was performed. The results showed safflor yellow A could enter the Nrf2 binding pocket of Keap1 Kelch domain (Fig. 6A), and the formation of safflor yellow A-Keap1 complex was driven by hydrogen bonds with the amino acid residues of Keap1 including LEU365 (2.2 Å), ASN382 (2.1 Å), ASN414 (1.9 Å), ARG415 (2.0, 2.3 and 2.3 Å), ILE416 (2.5 Å), ALA510 (2.1 Å), and SER602 (2.6 Å) (Fig. 6B). In addition, a 2D diagram also presented Van der Waals force and electrostatic interaction involved in the interaction between Keap1 and safflor yellow A (Fig. 6C).

Discussion

Acute lung injury/acute respiratory distress syndrome is characterized as pulmonary edema and acute inflammation, and recent COVID-19 pandemic has resulted in the increasing occurrence of ALI/ARDS rapidly (Habashi et al. 2021). LPS, a major component in Gram-negative bacteria, has
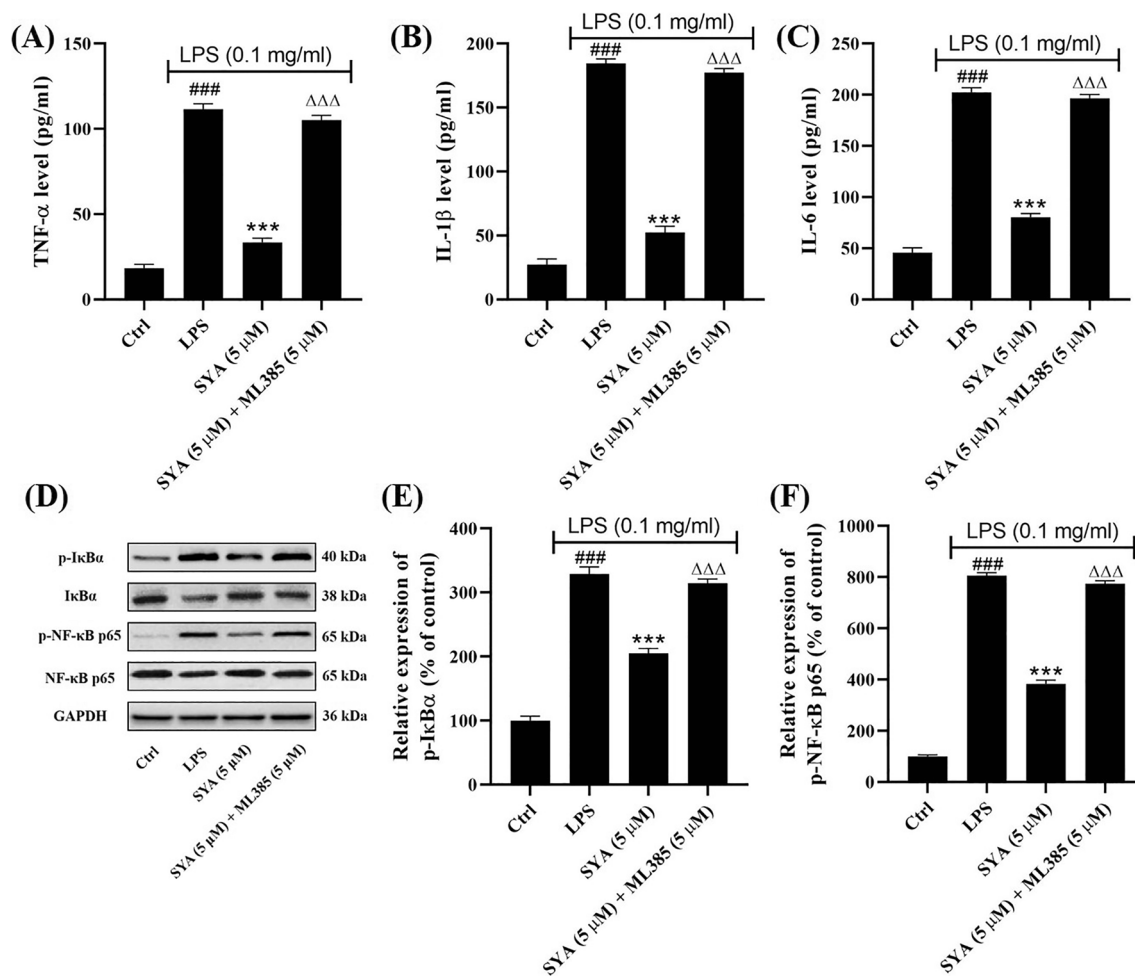
Fig. 3 Effects of safflor yellow A (**1**) on inflammation resulted from LPS in Beas-2B cells. **A–C** ELISA for the levels of TNF-α, IL-1β, and IL-6. **D** Western blot analysis for p-IκBα and p-NF-κB. **E, F** Densitometric analysis for p-IκBα and p-NF-κB. $n = 3$, ###$p < 0.001$ vs control group, ***$p < 0.001$ vs LPS group, ΔΔΔ$p < 0.001$ vs SYA group

been used to induce ALI/ARDS (Chen et al. 2010). Herein, we have found LPS reduced the viability of Beas-2B cells via induction of apoptosis. Safflor yellow A can significantly improve the poor cell viability.

In the pathogenesis of ALI/ARDS, inflammation plays the pivotal role (Butt et al. 2016). It was found that some pro-inflammatory cytokines such as TNF-α, IL-1β, and IL-6 have been elevated in patients with ALI/ARDS (Janz and Ware 2013). Herein, we found LPS can promote the secretion of TNF-α, IL-1β, and IL-6 while safflor yellow A could mitigate the excessive synthesis of these cytokines, which indicated its anti-inflammatory effects in Beas-2B cells. More experimental evidences have disclosed activation of NF-κB signaling pathway was involved in ALI/ARDS (Cao et al. 2018; An et al. 2021), which could regulate the secretion of these pro-inflammatory cytokines in transcription (Hayden and Ghosh 2011). Under unstressed conditions, NF-κB dimers are bound to IκBα to form the complex and

sequestered in cytosol (Oeckinghaus et al. 2011). In stimulated cells, IκBα is degraded through phosphorylation and following ubiquitination, which results in the phosphorylation of NF-κB dimers. Then the phosphorylated NF-κB will translocate into the nucleus and regulate the transcription of target genes (Yi et al. 2013). In the present investigation, it was observed safflor yellow A reduced the active IκBα and NF-κB, which indicated NF-κB signaling pathway was inhibited herein.

Oxidative stress occurs in humans during the progression of ALI/ARDS and aggravates pulmonary injury (Ward 2010). ROS can upregulate the expression of pro-inflammatory cytokines and mediate the inflammatory injury (Kellner et al. 2017). Meanwhile, excessive ROS can induce apoptosis (Simon et al. 2000). However, there are some antioxidant enzymes that can attenuate oxidative stress. For instance, SOD can catalyze superoxide as one of ROS to be hydrogen peroxide, which is decomposed to water by CAT or GSH Px

Fig. 4 Effects of safflor yellow A (**1**) on apoptosis of Beas-2B cells induced by LPS. **A** Western blot analysis for cleaved caspase-3, Bcl-2, and Bax. **B–D** Densitometric analysis for cleaved caspase-3, Bcl-2, and Bax. $n = 3$, $^{###}p < 0.001$ vs control group, $^{***}p < 0.001$ vs LPS group, $^{\Delta\Delta\Delta}p < 0.001$ vs SYA group
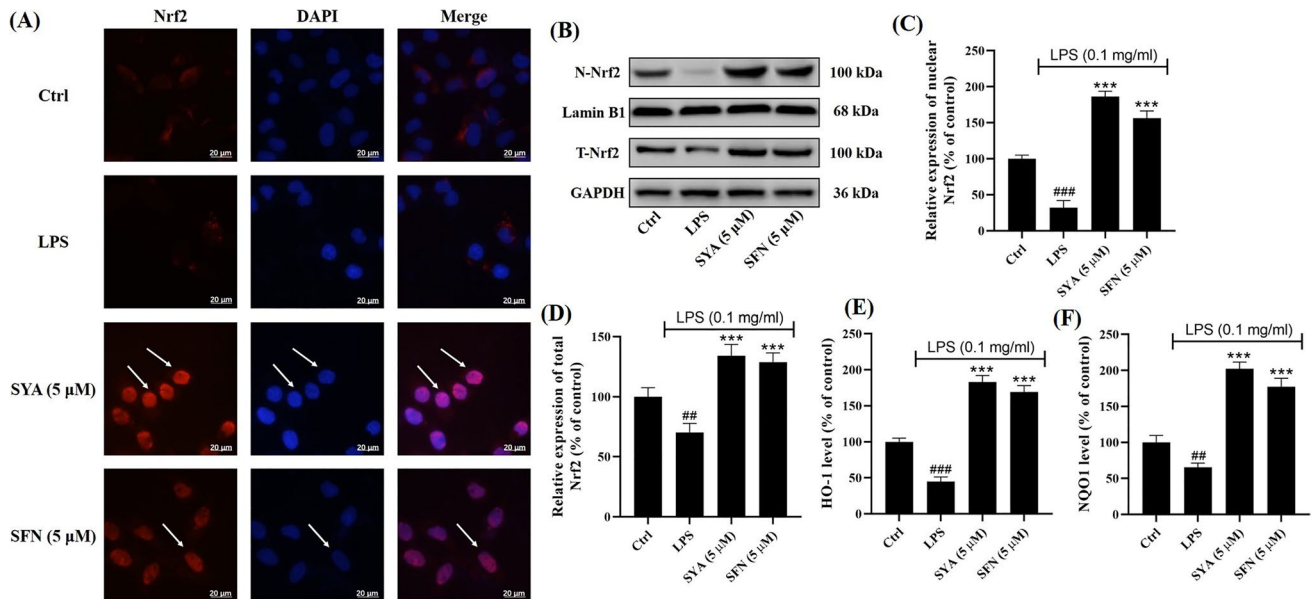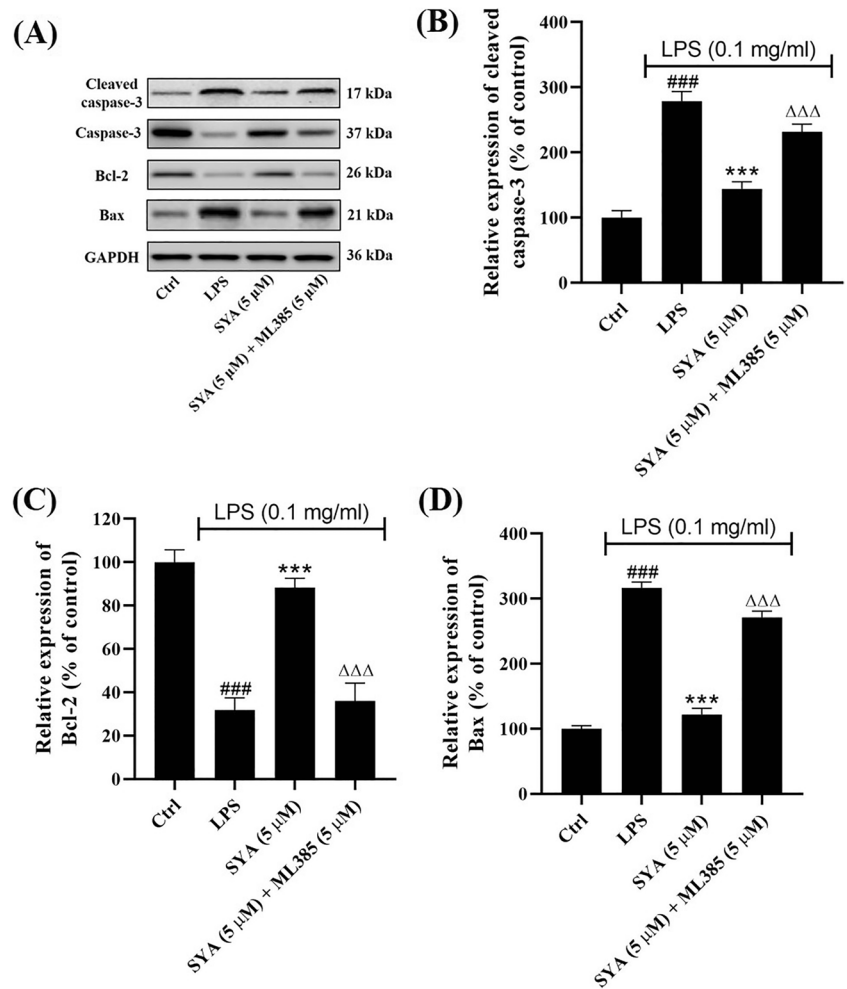
Fig. 5 Safflor yellow A (**1**) activated Nrf2 in Beas-2B cells injured by LPS. **A** Immunofluorescence assay for Nrf2. **B** Western blot analysis for nuclear and total Nrf2. **C**, **D** Densitometric analysis for nuclear and total Nrf2. **E**, **F** ELISA for HO-1 and NQO1. $n = 3$, $^{##}p < 0.01$ and $^{###}p < 0.001$ vs control group, $^{***}p < 0.001$ vs LPS group
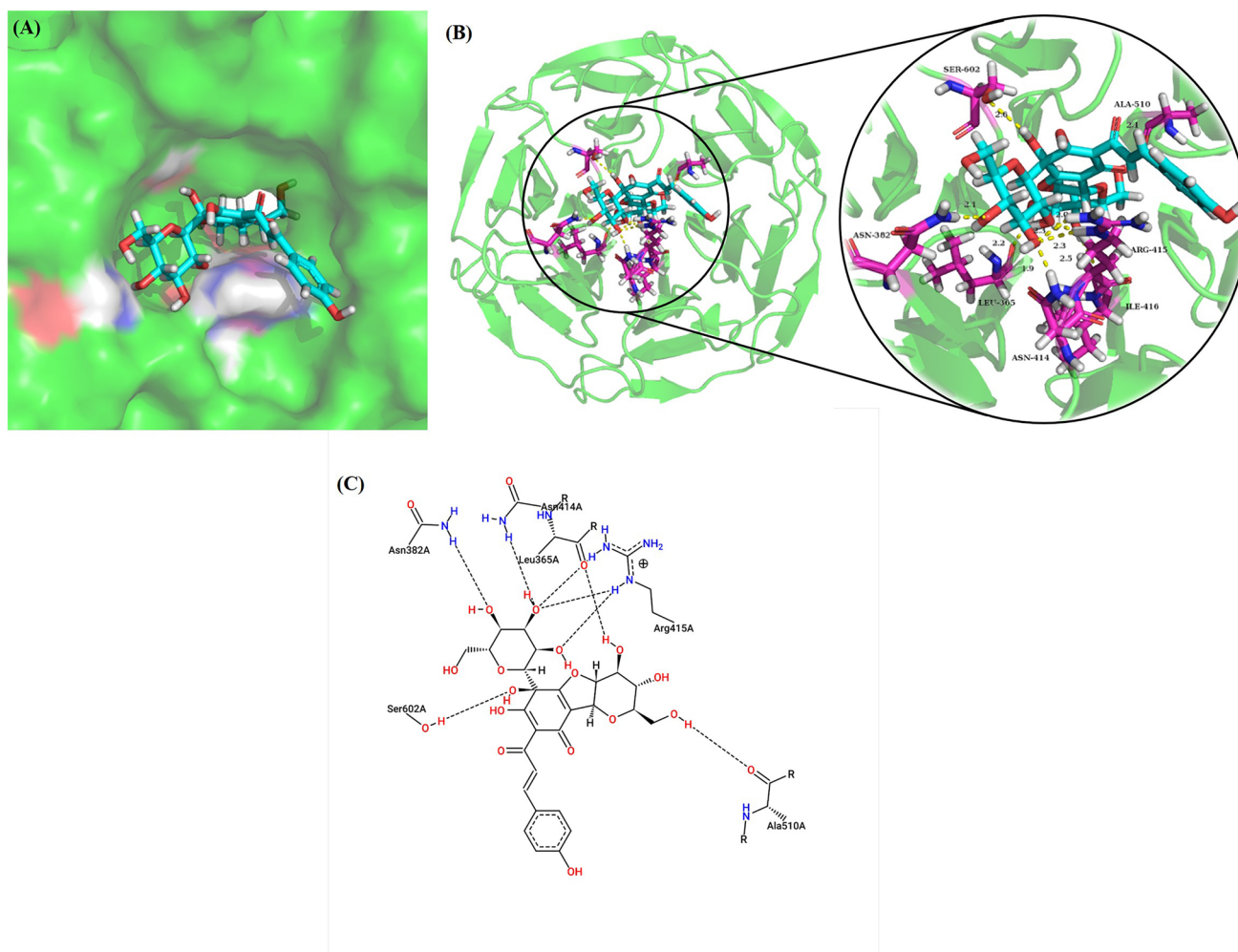
Fig. 6 Binding mode of safflor yellow A (**1**) with Keap1. **A** Binding pose of safflor yellow A (in cyan) in the Nrf2 binding cavity of Keap1. **B** 3D diagram for the interaction between amino acid residues (in magenta) and safflor yellow A (in cyan) via hydrogen bonds (yellow dashes). **C** 2D diagram for the interaction between Keap1 and safflor yellow A

(Dröge 2002). Herein, it was observed safflor yellow A suppressed the overproduction of ROS and MDA, the product of lipid peroxidation in LPS-stimulated Beas-2B cells. At the same time, the decreased activity of SOD, CAT, and GSH Px resulting from LPS stimulation has been improved in the presence of safflor yellow A. These results manifest safflor yellow A inhibits oxidative stress induced by LPS in Beas-2B cells.

Apoptosis is observed during ALI/ARDS as a response to inflammation (Chopra et al. 2009). In apoptosis, caspase-3 is an executioner enzyme affording the morphological changes of apoptotic cells, which is activated through cleavage at aspartic acid and serine residues (Budihardjo et al. 1999). As the members of Bcl-2 family, Bcl-2 is anti-apoptotic while Bax is pro-apoptotic (Youle and Strasser 2008). Bax can promote apoptosis via the formation of homodimers but it can bind to Bax to inhibit apoptosis (Tsujimoto 2003). In our investigation, though LPS resulted in the caspase-3 activation, upregulation of Bax, and downregulation of Bcl-2, safflor

yellow A could inactivate caspase-3, upregulate Bcl-2, and downregulate Bax. These observations indicated safflor yellow A inhibited apoptosis of Beas-2B cells induced by LPS.

As the transcription factor, Nrf2 can enhance the expression of antioxidant enzymes in transcription to defend oxidative stress (Bellezza et al. 2018). At the same time, activated Nrf2 can attenuate inflammation via increasing HO-1, elevating oxidative defense, and decreasing IκBα degradation (Madden and Itzhaki 2020). Without Nrf2 activators, two Keap1 monomers will form homodimer and bind to Nrf2 using their DLG and ETGE motifs in the Kelch domains, respectively (Ahmed et al. 2017). Since the affinity of DLG is lower than ETGE, it is easier for Nrf2 activators to interact with Keap1 at DLE motif than ETGE, which makes up the "hinge and latch" model (Tong et al. 2007). Therefore, oxidants or electrophiles will occupy the binding sites of DLE in Kelch domains and hinder the Nrf2-Keap1 interaction, which results in that de novo translated Nrf2 will not

undergo ubiquitination and degradation facilitated by Keap1, and freely translocate into nuclei. Herein we have found Nrf2 activation in Beas-2B cells induced by LPS in the presence of safflor yellow A. The protective effects of safflor yellow A against oxidative stress, inflammatory response, and apoptosis were closely associated whit Nrf2 activation, which was validated when introducing ML385, a Nrf2 inhibitor. The detailed interaction between safflor yellow A and Keap1 was revealed by molecular docking. Hydrogen bonds, Van der Waals force, and electrostatic interaction were the major forces to contribute the formation of complex. In addition, electrophiles can interact with the critical cysteine thiolate (soft base) groups in Keap1 and consequently suppress the ubiquitination of Nrf2 (Magesh et al. 2012). As soft Lewis acids, Michael acceptors are typical electrophiles. From the structure of safflor yellow A, there is an α,β-unsaturated carbonyl moiety as the classical Michael acceptor, which may also contribute to the activation of Nrf2 through disrupting the Nrf2-Keap1 interaction.

Conclusion

Collectively, we have evaluated the protective effects of safflor yellow A and explored the underlying mechanisms. Safflor yellow A can attenuate oxidative stress, ameliorate inflammation, and inhibit apoptosis in Beas-2B cells injured by LPS. Further investigations unraveled these effects were closely associated with Nrf2 activation via interaction with Keap1.

Declarations

Conflict of Interest The authors declare no competing interests.

Ethical Approval Not applicable.

Informed Consent Not applicable.

References

Ahmed SM, Luo L, Namani A, Wang XJ, Tang X (2017) Nrf2 signaling pathway: pivotal roles in inflammation. Biochim Biophys Acta Mol Basis Dis 1863:585–597. https://doi.org/10.1016/j.bbadis.2016.11.005

An N, Yang T, Zhang XX, Xu MX (2021) Bergamottin alleviates LPS-induced acute lung injury by inducing SIRT1 and suppressing NF-κB. Innate Immun 27:543–552. https://doi.org/10.1177/17534259211062553

Bacchetti T, Morresi C, Bellachioma L, Ferretti G (2020) Antioxidant and pro-oxidant properties of *Carthamus tinctorius*, hydroxy safflor yellow A, and safflor yellow A. Antioxidants 9:119. https://doi.org/10.3390/antiox9020119

Bellezza I, Giambanco I, Minelli A, Donato R (2018) Nrf2-Keap1 signaling in oxidative and reductive stress. Biochim Biophys Acta Mol Cell Res 1865:721–733. https://doi.org/10.1016/j.bbamcr.2018.02.010

Bryan HK, Olayanju A, Goldring CE, Park BK (2013) The Nrf2 cell defence pathway: Keap1-dependent and -independent mechanisms of regulation. Biochem Pharmacol 85:705–717. https://doi.org/10.1016/j.bcp.2012.11.016

Budihardjo I, Oliver H, Lutter M, Luo X, Wang X (1999) Biochemical pathways of caspase activation during apoptosis. Annu Rev Cell Dev Biol 15:269–290. https://doi.org/10.1146/annurev.cellbio.15.1.269

Butt Y, Kurdowska A, Allen TC (2016) Acute lung injury: a clinical and molecular review. Arch Pathol Lab Med 140:345–350. https://doi.org/10.5858/arpa.2015-0519-RA

Cao C, Yin C, Shou S, Wang J, Yu L, Li X, Chai Y (2018) Ulinastatin protects against LPS-induced acute lung injury by attenuating TLR4/NF-κB pathway activation and reducing inflammatory mediators. Shock 50:595–605. https://doi.org/10.1097/SHK.0000000000001104

Chen H, Bai C, Wang X (2010) The value of the lipopolysaccharide-induced acute lung injury model in respiratory medicine. Expert Rev Respir Med 4:773–783. https://doi.org/10.1586/ers.10.71

Chopra M, Reuben JS, Sharma AC (2009) Acute lung injury: apoptosis and signaling mechanisms. Exp Biol Med 234:361–371. https://doi.org/10.3181/0811-MR-318

Cuadrado A, Rojo AI, Wells G, Hayes JD, Cousin SP, Rumsey WL, Attucks OC, Franklin S, Levonen AL, Kensler TW, Dinkova-Kostova AT (2019) Therapeutic targeting of the NRF2 and KEAP1 partnership in chronic diseases. Nat Rev Drug Discov 18:295–317. https://doi.org/10.1038/s41573-018-0008-x

Dröge W (2002) Free radicals in the physiological control of cell function. Physiol Rev 82:47–95. https://doi.org/10.1152/physrev.00018.2001

Duan JL, Wang JW, Guan Y, Yin Y, Wei G, Cui J, Zhou D, Zhu YR, Quan W, Xi MM, Wen AD (2013) Safflor yellow A protects neonatal rat cardiomyocytes against anoxia/reoxygenation injury *in vitro*. Acta Pharmacol Sin 34:487–495. https://doi.org/10.1038/aps.2012.185

Fan EKY, Fan J (2018) Regulation of alveolar macrophage death in acute lung inflammation. Respir Res 19:50. https://doi.org/10.1186/s12931-018-0756-5

Galani V, Tatsaki E, Bai M, Kitsoulis P, Lekka M, Nakos G, Kanavaros P (2010) The role of apoptosis in the pathophysiology of acute respiratory distress syndrome (ARDS): an up-to-date cell-specific review. Pathol Res Pract 206:145–150. https://doi.org/10.1016/j.prp.2009.12.002

Habashi NM, Camporota L, Gatto LA, Nieman G (2021) Functional pathophysiology of SARS-CoV-2-induced acute lung injury and clinical implications. J Appl Physiol 130:877–891. https://doi.org/10.1152/japplphysiol.00742.2020

Hayden MS, Ghosh S (2011) NF-κB in immunobiology. Cell Res 21:223–244. https://doi.org/10.1038/cr.2011.13

Imai Y, Kuba K, Neely GG, Yaghubian-Malhami R, Perkmann T, van Loo G, Ermolaeva M, Veldhuizen R, Leung YH, Wang H, Liu H, Sun Y, Pasparakis M, Kopf M, Mech C, Bavari S, Peiris JS, Slutsky AS, Akira S, Hultqvist M, Holmdahl R, Nicholls J, Jiang C, Binder CJ, Penninger JM (2008) Identification of oxidative stress

and Toll-like receptor 4 signaling as a key pathway of acute lung injury. Cell 133:235–249. https://doi.org/10.1016/j.cell.2008.02.043

Janz DR, Ware LB (2013) Biomarkers of ALI/ARDS: pathogenesis, discovery, and relevance to clinical trials. Semin Respir Crit Care Med 34:537–548. https://doi.org/10.1055/s-0033-1351124

Keleku-Lukwete N, Suzuki M, Yamamoto M (2018) An overview of the advantages of KEAP1-NRF2 system activation during inflammatory disease treatment. Antioxid Redox Signal 29:1746–1755. https://doi.org/10.1089/ars.2017.7358

Kellner M, Noonepalle S, Lu Q, Srivastava A, Zemskov E, Black SM (2017) ROS signaling in the pathogenesis of acute lung injury (ALI) and acute respiratory distress syndrome (ARDS). Adv Exp Med Biol 967:105–137. https://doi.org/10.1007/978-3-319-63245-2_8

Lee J, Jang J, Park SM, Yang SR (2021) An update on the role of Nrf2 in respiratory disease: molecular mechanisms and therapeutic approaches. Int J Mol Sci 22:8406. https://doi.org/10.3390/ijms22168406

Liu C, Xiao K, Xie L (2022) Progress in preclinical studies of macrophage autophagy in the regulation of ALI/ARDS. Front Immunol 13:922702. https://doi.org/10.3389/fimmu.2022.922702

Liu C, Xiao K, Xie L (2022) Advances in the use of exosomes for the treatment of ALI/ARDS. Front Immunol 13:971189. https://doi.org/10.3389/fimmu.2022.971189

Liu Q, Ci X, Wen Z, Peng L (2018) Diosmetin alleviates lipopolysaccharide-induced acute lung injury through activating the Nrf2 pathway and inhibiting the NLRP3 inflammasome. Biomol Ther 26:157–166. https://doi.org/10.4062/biomolther.2016.234

Madden SK, Itzhaki LS (2020) Structural and mechanistic insights into the Keap1-Nrf2 system as a route to drug discovery. Biochim Biophys Acta Proteins Proteom 1868:140405. https://doi.org/10.1016/j.bbapap.2020.140405

Magesh S, Chen Y, Hu L (2012) Small molecule modulators of Keap1-Nrf2-ARE pathway as potential preventive and therapeutic agents. Med Res Rev 32:687–726. https://doi.org/10.1002/med.21257

Mokrá D (2020) Acute lung injury - from pathophysiology to treatment. Physiol Res 69:S353-S366. https://doi.org/10.33549/physiolres.934602

Oeckinghaus A, Hayden MS, Ghosh S (2011) Crosstalk in NF-κB signaling pathways. Nat Immunol 12:695–708. https://doi.org/10.1038/ni.2065

Patangrao Renushe A, Kumar Banothu A, Kumar Bharani K, Mekala L, Mahesh Kumar J, Neeradi D, Durga Veera Hanuman D, Gadige A, Khurana A (2022) Vincamine, an active constituent of *Vinca rosea* ameliorates experimentally induced acute lung injury in Swiss albino mice through modulation of Nrf-2/NF-κB signaling cascade. Int Immunopharmacol 108:108773. https://doi.org/10.1016/j.intimp.2022.108773

Rojo de la Vega M, Dodson M, Gross C, Mansour HM, Lantz RC, Chapman E, Wang T, Black SM, Garcia JG, Zhang DD (2016) Role of Nrf2 and autophagy in acute lung injury. Curr Pharmacol Rep 2:91–101. https://doi.org/10.1007/s40495-016-0053-2

Shaw P, Chattopadhyay A (2020) Nrf2-ARE signaling in cellular protection: mechanism of action and the regulatory mechanisms. J Cell Physiol 235:3119–3130. https://doi.org/10.1002/jcp.29219

Simon HU, Haj-Yehia A, Levi-Schaffer F (2000) Role of reactive oxygen species (ROS) in apoptosis induction. Apoptosis 5:415–418. https://doi.org/10.1023/a:1009616228304

Takahashi Y, Miyasaka N, Tasaka S, Miura I, Urano S, Ikura M, Hikichi K, Matsumoto T, Wada M (1982) Constitution of two coloring matters in the flower petals of *Carthamus tinctorius* L. Tetrahedron Lett 23:5163–5166. https://doi.org/10.1016/S0040-4039(00)85786-X

Tong KI, Padmanabhan B, Kobayashi A, Shang C, Hirotsu Y, Yokoyama S, Yamamoto M (2007) Different electrostatic potentials define ETGE and DLG motifs as hinge and latch in oxidative stress response. Mol Cell Biol 27:7511–7521. https://doi.org/10.1128/MCB.00753-07

Torrente L, DeNicola GM (2022) Targeting NRF2 and its downstream processes: opportunities and challenges. Annu Rev Pharmacol Toxicol 62:279–300. https://doi.org/10.1146/annurev-pharmtox-052220-104025

Tsujimoto Y (2003) Cell death regulation by the Bcl-2 protein family in the mitochondria. J Cell Physiol 195:158–167. https://doi.org/10.1002/jcp.10254

Ward PA (2010) Oxidative stress: acute and progressive lung injury. Ann N Y Acad Sci 1203:53–59. https://doi.org/10.1111/j.1749-6632.2010.05552.x

Wu S, Liao X, Zhu Z, Huang R, Chen M, Huang A, Zhang J, Wu Q, Wang J, Ding Y (2022) Antioxidant and anti-inflammation effects of dietary phytochemicals: the Nrf2/NF-κB signalling pathway and upstream factors of Nrf2. Phytochemistry 204:113429. https://doi.org/10.1016/j.phytochem.2022.113429

Wu YX, Zeng S, Wan BB, Wang YY, Sun HX, Liu G, Gao ZQ, Chen D, Chen YQ, Lu MD, Pang QF (2021) Sophoricoside attenuates lipopolysaccharide-induced acute lung injury by activating the AMPK/Nrf2 signaling axis. Int Immunopharmacol 90:107187. https://doi.org/10.1016/j.intimp.2020.107187

Yamamoto M, Kensler TW, Motohashi H (2018) The KEAP1-NRF2 system: a thiol-based sensor-effector apparatus for maintaining redox homeostasis. Physiol Rev 98:1169–1203. https://doi.org/10.1152/physrev.00023.2017

Yi PF, Wu YC, Dong HB, Guo Y, Wei Q, Zhang C, Song Z, Qin QQ, Lv S, Wu SC, Fu BD (2013) Peimine impairs pro-inflammatory cytokine secretion through the inhibition of the activation of NF-κB and MAPK in LPS-induced RAW264.7 macrophages. Immunopharmacol Immunotoxicol 35:567–572. https://doi.org/10.3109/08923973.2013.822508

Youle RJ, Strasser A (2008) The BCL-2 protein family: opposing activities that mediate cell death. Nat Rev Mol Cell Biol 9:47–59. https://doi.org/10.1038/nrm2308

Zhang H, Fan LJ, Liu J, Zhu JQ, Tan TT, Li M, Zhou YL (2022) Safflor yellow A protects vascular endothelial cells from ox-LDL-mediated damage. J Recept Signal Transduct Res 42:52–59. https://doi.org/10.1080/10799893.2020.1843492

Zheng DS, Chen LS (2017) Triterpenoids from *Ganoderma lucidum* inhibit the activation of EBV antigens as telomerase inhibitors. Exp Ther Med 14:3273–3278. https://doi.org/10.3892/etm.2017.4883